

Evolutionary-Optimized Photonic Network Structure in White Beetle Wing Scales

Bodo D. Wilts,* Xiaoyuan Sheng, Mirko Holler, Ana Diaz, Manuel Guizar-Sicairos, Jörg Raabe, Robert Hoppe, Shu-Hao Liu, Richard Langford, Olimpia D. Onelli, Duyu Chen, Salvatore Torquato, Ullrich Steiner, Christian G. Schroer, Silvia Vignolini, and Alessandro Sepe*

Most studies of structural color in nature concern periodic arrays, which through the interference of light create color. The “color” white however relies on the multiple scattering of light within a randomly structured medium, which randomizes the direction and phase of incident light. Opaque white materials therefore must be much thicker than periodic structures. It is known that flying insects create “white” in extremely thin layers. This raises the question, whether evolution has optimized the wing scale morphology for white reflection at a minimum material use. This hypothesis is difficult to prove, since this requires the detailed knowledge of the scattering morphology combined with a suitable theoretical model. Here, a cryoptychographic X-ray tomography method is employed to obtain a full 3D structural dataset of the network morphology within a white beetle wing scale. By digitally manipulating this 3D representation, this study demonstrates that this morphology indeed provides the highest white retroreflection at the minimum use of material, and hence weight for the organism. Changing any of the network parameters (within the parameter space accessible by biological materials) either increases the weight, increases the thickness, or reduces reflectivity, providing clear evidence for the evolutionary optimization of this morphology.

Whiteness arises from the random scattering of incident light from disordered structures.^[1] Opaque white materials have to contain a sufficiently large number of scatterers and therefore usually require thicker, material-rich nanostructures than structural color arising from the coherent interference of light.^[2,3] In nature, bright white appearance arises from the dense arrays of pterin pigments in pierid butterflies,^[4] guanine crystals in spiders,^[5] or leucophore cells in the flexible skin of cuttlefish.^[6] A striking example of such whiteness is found in the chitinous networks of white beetles, e.g., *Lepidiota stigma* and *Cyphochilus* sp.^[7–9] Previous research investigating these beetle structures has shown that the chitinous network is one of the most strongly scattering materials in nature, and therefore the question arises whether this structure is evolutionary optimized for strong scattering while minimizing the

Dr. B. D. Wilts, X. Sheng, Prof. U. Steiner, Dr. A. Sepe
Adolphe Merkle Institute
University of Fribourg, Chemin des Verdiers
4, CH-1700 Fribourg, Switzerland
E-mail: bodo.wilts@unifr.ch; alessandro.sepe@unifr.ch

X. Sheng, S.-H. Liu, Dr. R. Langford
Department of Physics
University of Cambridge
JJ Thompson Avenue, CB3 0HE Cambridge, UK

Dr. M. Holler, Dr. A. Diaz, Dr. M. Guizar-Sicairos, Dr. J. Raabe
Swiss Light Source
Paul Scherrer Institute
CH-5232 Villigen, Switzerland
R. Hoppe
Institute of Structural Physics
Technische Universität Dresden
01062 Dresden, Germany
O. D. Onelli, Dr. S. Vignolini
Department of Chemistry
University of Cambridge
Lensfield Road, CB2 1EW Cambridge, UK


D. Chen, Prof. S. Torquato
Department of Chemistry
Princeton University
Princeton, NJ 08544, USA

Prof. C. G. Schroer
Deutsches Elektronen-Synchrotron DESY
Notkestr. 85, 22607 Hamburg, Germany

Prof. C. G. Schroer
Department of Physics
Universität Hamburg
Luruper Chaussee 149, 22761 Hamburg, Germany

© 2017 The Authors. Published by WILEY-VCH Verlag GmbH & Co. KGaA, Weinheim. This is an open access article under the terms of the Creative Commons Attribution License, which permits use, distribution and reproduction in any medium, provided the original work is properly cited.

The copyright line for this article was changed on 21 Aug 2017 after original online publication.

 The ORCID identification number(s) for the author(s) of this article can be found under <https://doi.org/10.1002/adma.201702057>.

DOI: 10.1002/adma.201702057

amount of employed material, thus reducing the weight of the organism. The brilliant white reflection from *Cyphochilus* beetles is assumed to be important for camouflage among white fungi and in a shady environment.

In contrast to periodic photonic materials, for which the optical response is straightforward to calculate, the reflection of light from such disordered network morphologies requires a detailed knowledge of local geometry.^[2,3,9,10] For these complex cases, the validity of the diffusion approximation is limited, since single scattering elements are difficult to be identified.^[7] To fully understand the correlation between the structure and (optical) properties of complex materials, the detailed real-space structure in combination with a suitable model unravels this relationship. In optics, these include finite-element modeling or finite-difference time-domain (FDTD) techniques, which can be employed for materials with arbitrary structures.^[11]

Distortion-free 3D imaging of biological tissue with sub-micrometer resolution in a large volume is cumbersome and often relies on destructive techniques, i.e., focused ion beam (FIB)- scanning electron microscopy (SEM) serial tomography or electron tomography.^[7,12] Multi-keV ptychographic X-ray computed tomography (PXCT)^[13] overcomes this limitation, achieving below 15 nm resolution in radiation-hard materials at room temperature.^[14] In radiation-sensitive materials, however, the PXCT resolution used to be much worse (>100 nm), limited by either radiation damage at room temperature or by drifts of the setup at cryogenic temperatures.^[15,16] Here, we use “OMNY” (“tOMography Nano crYo”, see the Supporting Information), an instrument that allows cryo-PXCT of biological

materials, overcoming these imaging limitations. Cryogenic conditions preserve the structure of the sample during the measurement time, and interferometric positioning control eliminates thermal drifts.^[17] We use OMNY to image single wing scales of the brilliant white beetle *Cyphochilus* sp. These measurements provide a full structural characterization of the network morphology within the scales, clearly demonstrating the power of cryo-PXCT to extract quantitative structural information from biological tissues in a noninvasive, damage-resistant fashion.

Cyphochilus beetles (Coleoptera: Scarabaeidae: Melolonthinae) occur widely across Southeast Asia. The entire exoskeleton of the beetle (Figure 1a) is patterned with single wing scales covering the else velvet black exocuticle, which can be clearly seen by optical microscopy (Figure 1b). Each scale spans $\approx 200\ \mu\text{m}$ in length and $\approx 60\ \mu\text{m}$ in width. These scales strongly scatter incident light, and the reflectance is more or less constant across the visible wavelength range (Figure S3 of the Supporting Information).^[7]

Closer inspection of the white scales using SEM reveals that the scale interior comprises a network of interconnected, chitinous fibers surrounded by air.^[7–9,18,19] Earlier interpretation of the optical response of the scales^[7,9] was hampered by the lack of artifact-free, 3D visualization of the complex chitinous cuticle structure, and claims concerning the evolutionary optimized white color of the beetle were therefore anecdotal.

To gain insight into the optical function of the scales, we investigated the wing scales using PXCT. A first attempt was aimed at reconstructing the network morphology inside the beetle scale using conventional room-temperature PXCT,^[20]

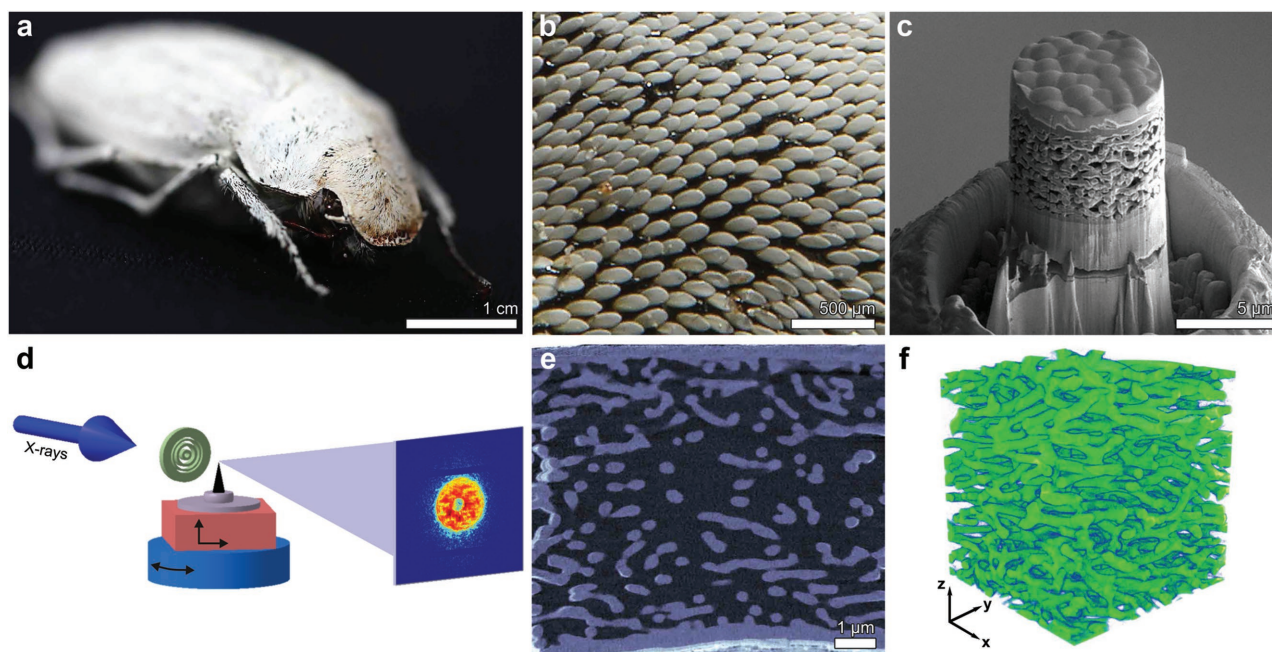


Figure 1. The brilliant white beetle *Cyphochilus* sp. a) Macrophotograph. b) Light micrograph of the scale arrangement on the beetle's elytra. c) Scanning electron micrograph of the sample pillar on a nanotomography pin holder obtained from a beetle scale by focused ion-beam milling. d) Sketch of the X-ray nanotomography setup. The sample is scanned and rotated through the beam (indicated by arrows) while recording the diffraction pattern (see the Supporting Information for more details). e) High-resolution tomographic slice (see Movies S2 and S3 of the Supporting Information), and f) 3D reconstruction of a $7 \times 7 \times 7\ \mu\text{m}^3$ inset of the volume obtained by cryo-PXCT of the inner structure of a beetle wing scale.

achieving a 3D resolution of 70 nm. Significant sample deformation was observed by visually comparing projections recorded at the beginning and the end of the PXCT measurement at the same projection angle.

To overcome this critical issue, the nanotomography measurements were repeated, using another beetle scale, at 92 K. Cryogenic conditions dramatically reduced structural deformation caused by the measurement (see the Supporting Information), enabling an isotropic 3D resolution of 28 nm over a sample volume of $\approx 350 \mu\text{m}^3$, which hinges on the minimization of in situ sample deformation, a typical problem for organic materials. While still somewhat worse than that of other techniques, e.g., serial transverse sectioning and imaging using transmission electron microscopy or X-ray crystallography, cryo-PXCT is noninvasive and does not rely on complicated embedding and/or staining protocols.

The spectral properties of the beetles are particularly interesting as they provide a very efficient incoherent broadband reflector with a comparable whiteness of common white paper but with a thickness of only about 1/10 of a typical paper sheet.^[7–9,19] To understand the key parameters governing this unusually strong scattering strength, the rendered 3D network of Figure 1f can be directly used to perform FDTD simulations of the structure's optical response to incident white light. The strength of this approach lies, i.e., in the ability to digitally modify the network morphology displayed in Figure 1f to test the changes in optical reflectivity.

The FDTD modeling results, Figure 2a, show that the reflectance strongly depends on the orientation of the network volume. The reflectance is significantly higher for the typical orientation of the scale (in-plane) and reaches a peak reflectance of ≈ 0.65 , while orientations perpendicular (out-of-plane) to the scale normal are significantly less reflective, with reflectances of ≈ 0.5 . This confirms previous results by Cortese et al.,^[8] which showed that the time-of-flight of a laser pulse through the structure is strongly anisotropic.

To further elucidate the nature of the optical anisotropy and its possible function, the network structure was digitally stretched and compressed. Figure 2b shows that compression along the z-axis lowers the in-plane reflectance. Stretching of the structure, i.e., making it more isotropic, results only in a slightly increased reflectance (0.69 vs 0.65). This indicates that the scales' structural anisotropy reduces the thickness needed to produce strong scattering resulting in the

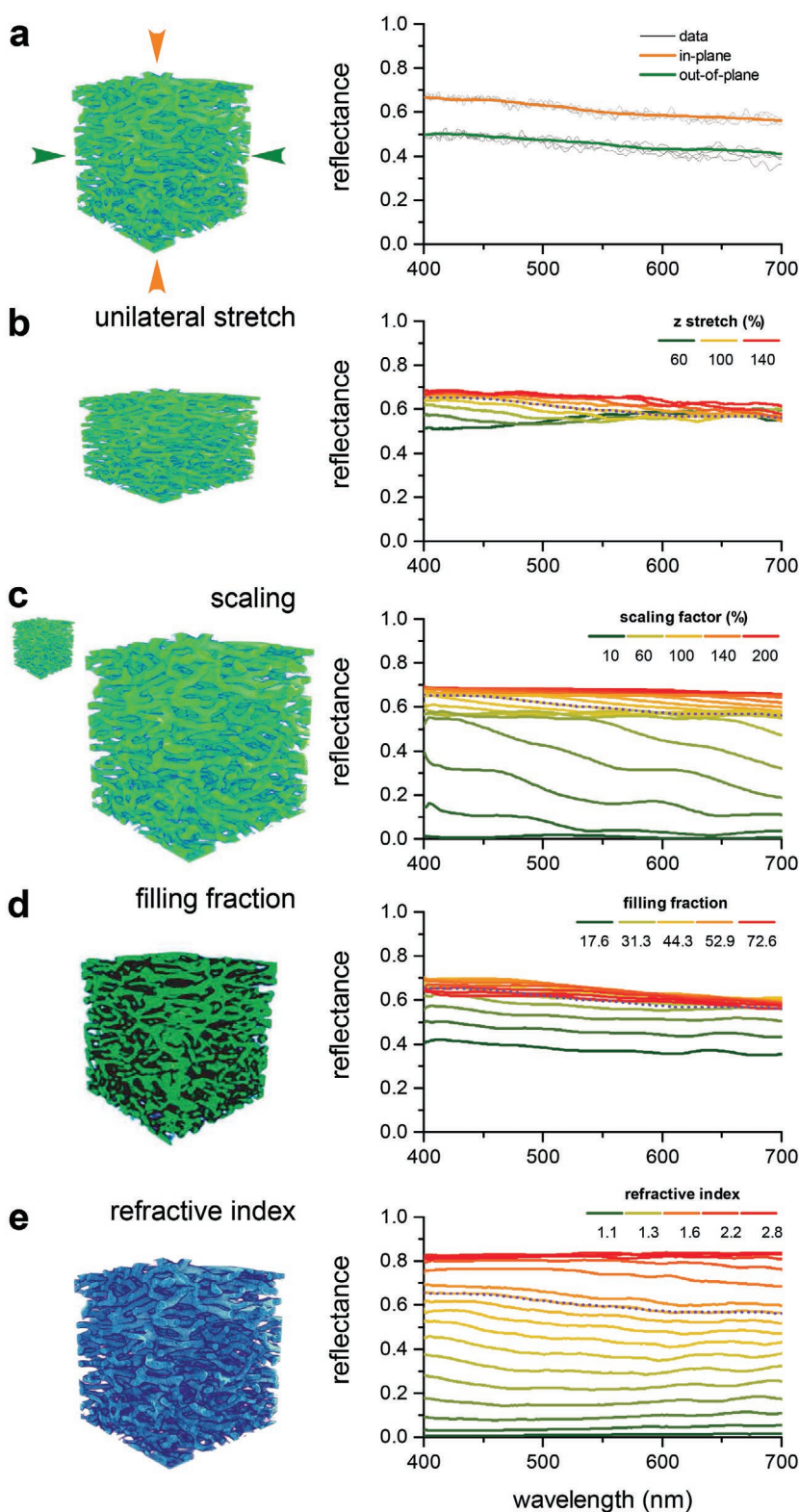


Figure 2. Spectrally resolved finite-difference time-domain (FDTD) simulations of light reflection (right column) from the network morphologies shown in the left column. a) Comparison of in-plane and out-of-plane optical directions of the cryo-PXCT-determined morphology (Figure 1f). Reflectance as a function of b) unidirectional stretching/compression of the structure along the z-axis; c) affine scaling of the network; d) filling fraction of the network struts; e) refractive index of the material comprising the network. The dotted lines correspond to the cryo-PXCT determined structure of Figure 1f for the (common) in-plane orientation.

observed brilliant whiteness. The scale thickness is functionally important for flying insects, as larger structures embedded on the wing require more material along the elytra.

By affinely expanding or contracting the network morphology, it is possible to test whether the scale structure has an optimized volume distribution of scatterers that maximize broadband reflectivity (Figure 2c). Uniform compression along all spatial directions results in a severe reduction of the reflectivity, which eventually (below 20% of the original size) disappears all together, i.e., the material becomes transparent. This result is unsurprising since for a distribution of scattering centers which is comparable to the incident wavelength, propagating light “averages” over its discrete structure, entering the “optical crowding” or “effective medium” regime.^[21] Uniform expansion of the network morphology changes the broadband reflectance very little. This result again indicates that the structure is optimized for achieving maximal whiteness for a minimal scale thickness.

The weight of the scale is also affected by the porosity of the network morphology and therefore the strut thickness. The reconstructed morphology of Figure 1f has a solid content (filling fraction) of $45 \pm 6\%$. Figure 2d explores the optical response of the network morphology upon digitally enlarging and reducing the strut diameter, which alters the filling fraction. Optimal broadband reflection was found for a rather broad filling-fraction range, from ≈ 40 to 70%. The filling fraction of the beetle scales of $\approx 45\%$ lies at the lower end of this range, again indicating an optimization that maximizes scattering power for a minimum of material use.

Fundamentally, the scattering power in single and multiple scattering systems depends strongly on the refractive index. While biological organisms have limited access to high refractive index materials, it is interesting to explore the variation of the network reflectivity for different, synthetically available refractive indices. In Figure 2e, the refractive index was varied from $n = 1.1$ to $n = 2.8$, where the void space of the network was modeled as air with $n_{\text{air}} = 1$. While, unsurprisingly, higher refractive indices result in a stronger average reflectance, up to 84% for $n = 2.8$ (i.e., close to that of rutile titanium dioxide, a synthetic dielectric material commonly employed in photonic applications^[22]), the broadband reflectivity rapidly decays for $n < 1.6$. Given the fact that the refractive index of chitin, varying from 1.6 to 1.55 (blue to red wavelengths, respectively), is among the highest found for purely organic biological materials,^[23,24] this simulation illustrates yet another aspect of optical optimization of the network morphology.

The careful balance of structural parameters described above begets the question whether the random network morphology exhibits hidden correlations that optimize the scattering of incident light. This question is motivated by the consideration that the optimization of the scattering strength requires an average distance between scatterers just above the wavelength of visible light (to avoid optical crowding) and the absence of periodic order (to avoid a photonic bandgap^[25,26]). An established example of such hidden correlations is “hyperuniformity,” which refers to the anomalous suppression of density fluctuations at large length scales.^[27–29] Hyperuniform systems include all perfect spatially periodic patterns and special disordered

systems. To date, disordered hyperuniformity has been discovered in only a small number of biological and physical systems,^[28] including the arrangement of color-sensing photoreceptors in avian retinae^[30] and designed 2D photonic materials.^[29]

The high-resolution cryo-PXCT data of Figure 1f enable a direct structural analysis and to test the data for hidden correlations. Using a medial axis analysis,^[31] the distribution of lengths and widths of the individual struts forming the network structure was analyzed (Figure 3a–c). Both parameters show very broad distributions of 1105 ± 360 nm (mean \pm full width at half maximum) and 115 ± 80 nm, respectively, which are typical for random network structures.

To investigate whether this seemingly random morphology has hidden structural correlations, e.g., hyperuniformity, the spectral density $\tilde{\chi}_k$ in the various planes of the Fourier space of the network structure was calculated. The scaled spectral density profiles along the two main directions (out-of-plane and in-plane of the beetle scale) are shown in Figure 3d,e. The density profile is strongly dependent on the direction of investigation, indicating a strong structural anisotropy of the network (cf. Figure 1b). While the spectral densities in the two out-of-plane directions, x – z and y – z , show strong directional dependence (Figure 3d), the spectral density in the in-plane direction, x – y , is largely isotropic (Figure 3e). Along the out-of-plane direction, the structure seems to be “layer-like” with a pseudolayer distance of ≈ 270 nm. The anisotropy of the nanostructure can be further quantified by the quantity $\xi = \frac{\tilde{\chi}(0,0,k_z \rightarrow 0)}{\tilde{\chi}(k_x \rightarrow 0, k_y \rightarrow 0, 0)} - 1$, where $\tilde{\chi}(0,0,k_z \rightarrow 0)$ and $\tilde{\chi}(k_x \rightarrow 0, k_y \rightarrow 0, 0)$ are extrapolated values of the spectral density in the z -direction and x – y plane as \mathbf{k} approaches 0 and $\tilde{\chi}(k_x, k_y, k_z) \equiv \tilde{\chi}(\mathbf{k})$. For isotropic structures, ξ should be 0 and increase for increasing structural anisotropy. In the case of the investigated structure, ξ is in the order of 10, indicating a strong structural anisotropy. Figure 3d,e moreover illustrates that the network morphology is not strictly hyperuniform, since $\tilde{\chi}_k$ does not vanish as the wavenumber k approaches 0 from any direction. This fact is further corroborated by investigating the local variation of the volume fraction of scatterers as a function of a spherical probe of radius R . Figure 3f shows that the scaled local volume fraction variance $R^3\sigma^2(R)$ varies linearly with R and plateaus for large R . Hyperuniformity requires a faster decay of $\sigma^2(R)$ for $R \rightarrow \infty$.^[28,32] The results of Figure 3 therefore clearly demonstrate the absence of hyperuniformity and that the two size distributions of Figure 3b,c are close to Gaussian. In addition, we have employed a variety of other structural descriptors to spatially characterize the beetle ultrastructure, as detailed in the Supporting Information.

In summary, we have employed a new experimental technique, cryo-PXCT, to study the nanostructured photonic system of the *Cyphochilus* beetle. The combination of cryo-PXCT structural reconstruction with sub-30 nm resolution with FDTD modeling allowed us to demonstrate that the 3D network morphology of the beetle is carefully optimized by evolution. This is achieved by the judicious simultaneous selection of four parameters, the selection of (1) the correct network density, (2) the optimal fill fraction, (3) one of the biologically highest refractive indices for transparent materials, and (4) a beneficial

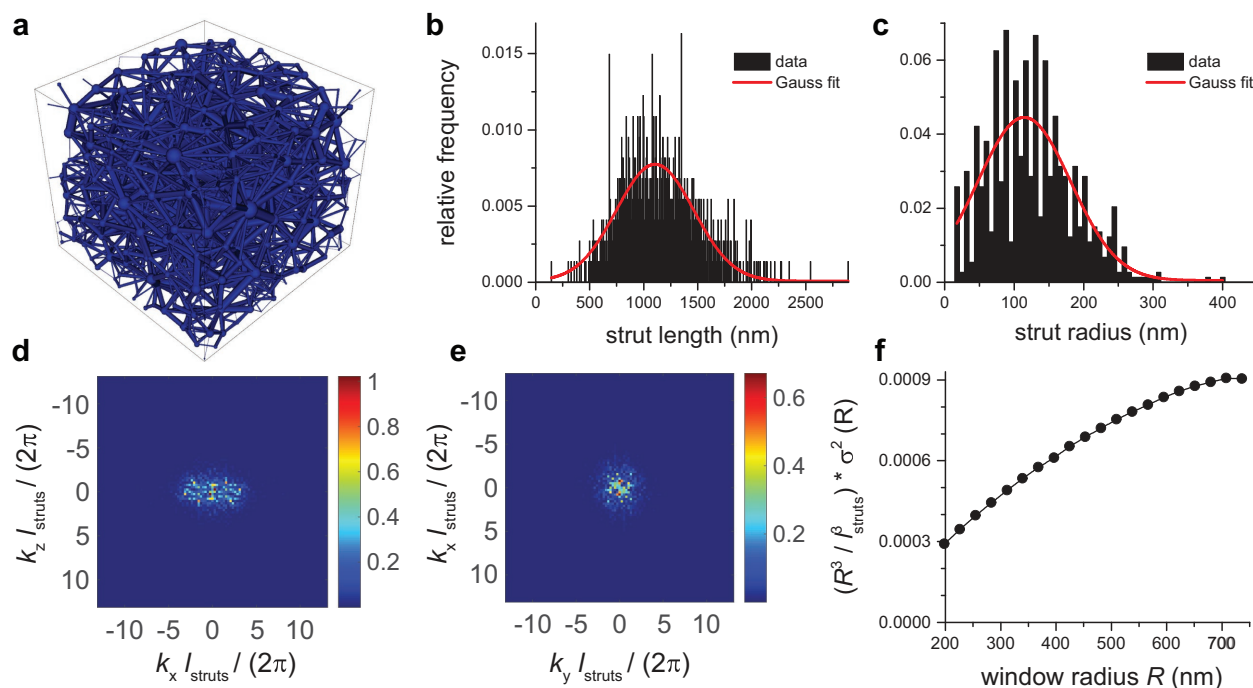


Figure 3. Structural analysis of the reconstructed photonic structure. a) Sketch of the medial axis representation of the network. b,c) Size statistics of the b) strut length and c) width, respectively. d,e) Scaled spectral density $\tilde{\chi}_k$ of the network along two characteristic planes in the Fourier space d) parallel and e) perpendicular to the structure normal. f) Scaled local volume fraction as a function of the window radius R . In this representation, a linear decay for $R \rightarrow \infty$ is indicative of a random distribution.

structural anisotropy. Changing any of these parameters may improve one of the decisive properties (e.g., reflectivity), but always at the expense of the other (e.g., used material per unit area). In particular, the digital variation of these four network parameters in Figure 2 does confirm the optimized nature of the photonic network morphology that maximizes the white broadband reflectivity while minimizing the materials use (and hence weight) per unit area.

Metabolically, the production of the wing scale material is considerable, given its relatively large thickness of $\geq 7 \mu\text{m}$. Each beetle wing scale, similar to the wing scales of butterflies, develops from a single differentiating cell,^[33] most likely through prestretching of internal F-actin filaments and subsequent external deposition of chitinous cuticle. 3D structures in arthropods are often highly ordered^[26,34,35] and the precise mechanism driving structure formation is still an open debate. While some work exists on periodic morphologies in butterfly wing scales,^[33,35] structure formation of disordered networks in developing wing scale cells is up to now uninvestigated.

While the optimization of materials use is evidently essential for flying insects, it presents a bioinspired design strategy for the manufacture of white reflectors, particularly in applications in which the use of low refractive index organic materials is desirable, e.g., the food industry. Additionally, the use of higher refractive index materials allows us to even further improve the scattering strength of similar network materials while minimizing materials use and weight of the coating.

Supporting Information

Supporting Information is available from the Wiley Online Library or from the author.

Acknowledgements

B.D.W. and X.S. contributed equally to this work. The authors thank Frank Scheffold, Nicolas Müller, Andreas Menzel, and Oliver Bunk for fruitful discussions; Demet Asil, Reza Saberi Moghaddam, Eric Tapley, and Jon J. Rickard for help with experiments; Charly Rappo for the permission to use the photograph of Figure 1a; and Holger Averdunk for help with the medial axis representation. PXCT measurements were performed at the cSAXS beamline at the Swiss Light Source, Paul Scherrer Institut, Switzerland. The OMNY instrumentation was supported by the Swiss National Science Foundation SNSF (Funding scheme RQUIP, Project number 145056). This research was financially supported through the National Centre of Competence in Research *Bio-Inspired Materials*, the Adolphe Merkle Foundation (to B.D.W. and U.S.), a BBSRC David Phillips fellowship (BB/K014617/1), the European Research Council (ERC-2014-STG H2020 639088, to O.O. and S.V.), and the Ambizione program of the Swiss National Science Foundation SNSF (168223, to B.D.W.). The authors acknowledge support from the Winton Programme for the Physics of Sustainability. B.D.W., U.S., A.S., and S.V. conceived the research project. X.S., S.-H.L., R.L., O.D.O., and S.V. prepared the samples. X.S., M.H., A.D., M.G.-S., J.R., R.H., C.G.S., and A.S. participated in the X-ray experiments. A.D. and M.G.-S. analyzed the X-ray data toward 3D reconstructions. B.D.W. performed FDTD simulations. D.C., B.D.W., and S.T. performed statistical analysis of the structure. B.D.W., U.S., and A.S. wrote the paper with contributions from all authors.

Conflict of Interest

The authors declare no conflict of interest.

Keywords

arthopods, biophotonic structures, light scattering, nanotomography, X-ray ptychography

Received: April 12, 2017

Revised: May 19, 2017

Published online: June 22, 2017

- [1] D. S. Wiersma, *Nat. Photonics* **2013**, 7, 188.
- [2] M. Srinivasarao, *Chem. Rev.* **1999**, 99, 1935.
- [3] S. Kinoshita, S. Yoshioka, J. Miyazaki, *Rep. Prog. Phys.* **2008**, 71, 076401.
- [4] B. D. Wilts, B. Wijnen, H. L. Leertouwer, U. Steiner, D. G. Stavenga, *Adv. Opt. Mater.* **2017**, 5, 1600879.
- [5] A. Levy-Lior, E. Shimoni, O. Schwartz, E. Gavish-Regev, D. Oron, G. Oxford, S. Weiner, L. Addadi, *Adv. Funct. Mater.* **2010**, 20, 320.
- [6] L. M. Mäthger, S. L. Senft, M. Gao, S. Karaveli, G. R. R. Bell, R. Zia, A. M. Kuzirian, P. B. Dennis, W. J. Crookes-Goodson, R. R. Naik, G. W. Kattawar, R. T. Hanlon, *Adv. Funct. Mater.* **2013**, 23, 3980.
- [7] M. Burrelli, L. Cortese, L. Pattelli, M. Kolle, P. Vukusic, D. S. Wiersma, U. Steiner, S. Vignolini, *Sci. Rep.* **2014**, 4, 6075.
- [8] L. Cortese, L. Pattelli, F. Utel, S. Vignolini, M. Burrelli, D. S. Wiersma, *Adv. Opt. Mater.* **2015**, 3, 1337.
- [9] P. Vukusic, B. Hallam, J. Noyes, *Science* **2007**, 315, 348.
- [10] S. Vignolini, T. Gregory, M. Kolle, A. Lethbridge, E. Moyroud, U. Steiner, B. J. Glover, P. Vukusic, P. J. Rudall, *J. R. Soc. Interface* **2016**, 13, 20160645.
- [11] B. D. Wilts, K. Michielsen, H. De Raedt, D. G. Stavenga, *Proc. Natl. Acad. Sci. USA* **2014**, 11, 4363.
- [12] J. W. Galusha, L. R. Richey, J. S. Gardner, J. N. Cha, M. H. Bartl, *Phys. Rev. E* **2008**, 77, 050904.
- [13] M. Dierolf, A. Menzel, P. Thibault, P. Schneider, C. M. Kewish, R. Wepf, O. Bunk, F. Pfeiffer, *Nature* **2010**, 467, 436.
- [14] M. Holler, M. Guizar-Sicairos, E. H. Tsai, R. Dinapoli, E. Müller, O. Bunk, J. Raabe, G. Aeppli, *Nature* **2017**, 543, 402.
- [15] A. Diaz, B. Malkova, M. Holler, M. Guizar-Sicairos, E. Lima, V. Panneels, G. Pigino, A. G. Bittermann, L. Wettstein, T. Tomizaki, O. Bunk, G. Schertler, T. Ishikawa, R. Wepf, A. Menzel, *J. Struct. Biol.* **2015**, 192, 461.
- [16] E. Lima, A. Diaz, M. Guizar-Sicairos, S. Gorelick, P. Pernot, T. Schleier, A. Menzel, *J. Microsc.* **2013**, 249, 1.
- [17] M. Holler, J. Raabe, *Opt. Eng.* **2015**, 54, 054101.
- [18] B. T. Hallam, A. G. Hiorns, P. Vukusic, *Appl. Opt.* **2009**, 48, 3243.
- [19] S. M. Luke, B. T. Hallam, P. Vukusic, *Appl. Opt.* **2010**, 49, 4246.
- [20] M. Holler, A. Diaz, M. Guizar-Sicairos, P. Karvinen, E. Färm, E. Härkönen, M. Ritala, A. Menzel, J. Raabe, O. Bunk, *Sci. Rep.* **2014**, 4, 3857.
- [21] D. J. Bergman, D. Stroud, *Solid State Phys.* **1992**, 46, 147.
- [22] X. Chen, S. S. Mao, *Chem. Rev.* **2007**, 107, 2891.
- [23] D. E. Azofeifa, H. J. Arguedas, W. E. Vargas, *Opt. Mater.* **2012**, 35, 175.
- [24] H. L. Leertouwer, B. D. Wilts, D. G. Stavenga, *Opt. Express* **2011**, 19, 24061.
- [25] S. R. Sellers, W. Man, S. Sahba, M. Florescu, *Nat. Commun.* **2017**, 8, 14439.
- [26] B. D. Wilts, K. Michielsen, H. De Raedt, D. G. Stavenga, *J. R. Soc. Interface* **2012**, 9, 1609.
- [27] S. Torquato, F. H. Stillinger, *Phys. Rev. E* **2003**, 68, 041113.
- [28] S. Torquato, *Phys. Rev. E* **2016**, 94, 022122.
- [29] M. Florescu, S. Torquato, P. J. Steinhardt, *Proc. Natl. Acad. Sci. USA* **2009**, 106, 20658.
- [30] Y. Jiao, T. Lau, H. Hatzikirou, M. Meyer-Hermann, J. C. Corbo, S. Torquato, *Phys. Rev. E* **2014**, 89, 022721.
- [31] A. Jones, A. Sheppard, R. Sok, C. Arns, A. Limaye, H. Averdunk, A. Brandwood, A. Sakellariou, T. Senden, B. Milthorpe, M. A. Knackstedt, *Physica A* **2004**, 339, 125.
- [32] S. Torquato, G. Zhang, F. Stillinger, *Phys. Rev. X* **2015**, 5, 021020.
- [33] H. Ghiradella, *J. Morphol.* **1989**, 202, 69.
- [34] V. Saranathan, A. E. Seago, A. Sandy, S. Narayanan, S. G. J. Mochrie, E. R. Dufresne, H. Cao, C. O. Osuji, R. O. Prum, *Nano Lett.* **2015**, 15, 3735.
- [35] B. D. Wilts, B. A. Zubiri, M. A. Klatt, B. Butz, M. G. Fischer, S. T. Kelly, E. Spiecker, U. Steiner, G. E. Schröder-Turk, *Sci. Adv.* **2017**, 3, e1603119.